NEW YORK UNIVERSITY

SCHOOL OF ENGINEERING AND SCIENCE

DEPARTMENT OF METEOROLOGY

AND OCEANOGRAPHY

NASA Grant NGL-33-016-013

Basic Research in Meteorology and Atmospheric Physics

Informal Report Covering the Period

December 1971 through May 1972

June 1972

Contents

ATMOSPHERIC TEMPERATURE SOUNDINGS BY RADIOMETERS ABOARD SATELLITES

by

Roger Opstbaum

Work has continued on a survey of the methods for sounding the atmospheric temperature profile by remote measurements. The mainstream of this survey deals with infrared inversion techniques. However, the emphasis for this six-month period has been placed in reviewing related topics: sounding in the microwave region of the spectrum, sounding in cloudy atmospheres, and measuring sea-surface temperatures remotely. This survey was suggested by Dr. Joseph S. Hogan to provide scientists at the Goddard Institute for Space Studies, who are developing a remote-sensing program for use with their dynamical models, with a compendium of previous research papers in the remote sensing field.

At the end of the previous six-month period, the survey, which had proceeded chronologically, had gotten as far as Wark and Fleming's (1966) empirical orthogonal method (explained in the previous report of this series). This appeared to be the most recent non-iterative approach to the problem. A number of papers in recent years have chosen a method along the lines of Chahine (1968). The Planck function $B[\nu,T(p)]$ found in the radiative transfer equation

$$I(\nu,\bar{p}) = \epsilon B\,[\nu,T(p_o)]\,\tau(\nu,p_o) + \int_{p_o}^{\bar{p}} B\,[\nu,T(p)\,\frac{2\tau(\nu,p)}{2p}\,dp \qquad (1)$$

in which I is radiation received at the satellite for wavenumber interval ν at pressure $\bar{p}$, ϵ is the emissivity of the lower boundary which is at pressure p_o, T is the absolute temperature and τ is the transmissivity, was often linearized in previous inversion schemes. Chahine, however, made use of the fact that the dependence of the transmission on the temperature was negligible in comparison to the dependence of the Planck function on temperature, and rather than seeking a linear form for equation (1), he was able to put it into the form

$$I(\nu,\bar{p}) = X\,[T(p_o)]\,A(\nu,p_o) + \int_{p_o}^{\bar{p}} X[T(p)]K(\nu,p)\,dp \qquad (2)$$

with "factors" X, A, and K. The above equation was solved for X(T) in simulation studies by creating a temperature profile $\bar{T}(p)$, determining its associated radiance profile, and then using the following iterative procedure to retrieve the temperature profile (quotes directly from Chahine, 1968):

1. "Select a set of ten sounding frequencies corresponding to ten pressure levels." Hogan (1972) advises me that numerical experiments have shown that due to the overlapping of the atmospheric weighting functions for carbon dioxide, in practice only 5 or 6 independent sounding frequencies can be chosen.

2. "Make an initial guess $T^{\circ}(p)$ and solve equation 2; check the residuals R_i^n and (R^n) av, and satisfy convergence."

3. "Compare the results with the exact answer $\bar{T}(p)$." The results are interesting. The guess converges quite rapidly to a rather accurate solution. Also, each isothermal guess converges to the same solution after about 5 iterations. However, the uniqueness of this solution, or, for that matter, any solution, is still questionable, considering the nature of the weighting functions. The iterations have the effect of producing solutions which are accurate to only a few degrees from the actual profile.

Several papers dealing with microwave sensing have been included in the survey. Among them was the paper considered to be the pioneer paper in the field (Meeks and Lilley, 1963). This paper discussed results of calculations of opacity due to atmospheric oxygen in millimeter wavelengths and emphasized the complication of the radiative transfer in this region of the spectrum due to Zeeman splitting caused by the influence of the Earth's magnetic field. The paper also outlined a program to make the temperature measurements in the microwave region. Meanwhile, Staelin (1969) reviewed the work and applications of remote sensing in the microwave region. Among other important points made, he stated "microwave sensors provide the only remote sensing technique capable of measuring atmospheric temperature profiles in the presence of clouds." In view of the difficulty clouds present to people working in the field of infrared remote sensing, microwave temperature sensing will have to be given more emphasis and research than it has been given in the past.

This is clearly seen to be true when a paper is encountered which discusses clouds and their effects on infrared sensing. For example, House (1968) has tried to introduce clouds into King's (1964) nonlinear method. He concludes that accurate temperature soundings can only be made down to cloud-top level, a fact well established before his study.

Recognizing that clouds contaminate infrared data, Smith et al. (1970) have proposed a method for deleting cloudy data from a mixed data set for the purpose of making sea surface temperature measurements. The method can be termed a statistical-histogram method and it makes use of the fact that the brightness temperature for the clear atmosphere modal peak radiance is, statistically, the most

probable surface temperature. By collecting satellite data for a small latitudinal-longitudinal patch over a short period, a statistically random sample can be collected, which may or may not contain perfectly clear or cloudy data and probably contains some mixture of each, so that a "clear mode" can be established. The method was successful enough to be considered for operational use.

The survey is expected to be completed in the early fall.

ORBITAL DETECTION OF STRATOSPHERIC AEROSOLS

by

Gregory L. Matloff

Research currently underway includes a feasibility study of the orbital detection of aerosols in the lower stratosphere. This research is under the direction of Dr. J. Hansen of the Goddard Institute for Space Studies. It appears that such effects as Rayleigh (molecular) scattering and refraction can be accounted for and that occultation of stars by the Earth's atmosphere can be observed from satellites to determine local aerosol concentrations.

MONTHLY PRECIPITATION CHARTS FOR THE WORLD

by

Roger Opstbaum

Mean monthly precipitation charts have now been completed for all 12 months of the year. The data have been amassed from 6 sources (U.S. Department of Commerce, 1969a; U.S. Department of Commerce, 1969b; Critchfield, 1966; Miller and Thompson, 1970; Arakawa, 1969; and Wallen, 1970) and are plotted on a grid display according to latitude and longitude.

As has been discussed in previous reports, because of the lack of precipitation data for the ocean areas, these charts cannot be used for such purposes as a heat budget study for the Earth. However, the great density of data over land areas makes the precipitation study purposeful and desirable. Its potential utility has been discussed in previous reports.

The results confirm our previous general notions about global precipitation patterns. Furthermore, their detail over land areas and method of display shed some light on the mechanisms involved in seasonal and orographic causes of precipitation.

Global precipitation patterns can probably best be described as patchy, with the greatest areas of high precipitation located in the subtropics and tropics. These are semi-permanent regions and they follow the movement of the Inter-Tropical Convergence Zone rather closely, although not all of them are located at the ITCZ. These patterns are responsible for Tropical Rain Forest type climates.

Other precipitation types which are clearly illustrated in these charts are monsoonal (seasonal) and orographic precipitation mechanisms. The most striking example of a combination of both types of mechanisms can be found in the region around Cherrapunji, India. During the July monsoon, an average of greater than 2000 mm is recorded for that area, while in some winter months, the amount of precipitation recorded is less than that recorded in the eastern United States.

More permanent orographically-induced precipitation is found, for example, in the Pacific Northwest in the region of the Cascades where precipitation values persistently higher than the surrounding areas are recorded the year round. This annual condition is probably due to the prevailing westerly winds from the ocean in that region.

Most of the higher latitudes are not influenced by special topographic features and have a surprisingly constant amount of precipitation throughout the year, a condition more prevalent in the Northern Hemisphere than in the Southern Hemisphere. In the Southern Hemisphere, the transition from tropical to polar conditions is much more pronounced, possibly due to the large oceanic area, and this is reflected in precipitation amounts by a transition from heavy equatorial precipitation to the rather dry Antarctic continent.

There are also numerous semi-permanent and permanent desert areas. Many stations in the permanent deserts have an average of 0 mm for the entire year. It is rare, even in the cases of the semi-permanent deserts, for more than 50 mm precipitation to be recorded for one particular month in any desert region.

DETERMINATION OF THE CLOUD STRUCTURE OF A PLANET FROM REMOTE POLARIZATION MEASUREMENTS

by

Roger Opstbaum

A study has begun in which the polarization of radiation arriving at Earth from selected points on a distant planet is calculated. These calculations are performed for various phase angles, optical depths, and models of the distribution of the multiple scattering particles. These multiple scattering computations involve the doubling method (van de Hulst, 1963; Hansen, 1971) together with the

method of successive orders of scattering (Uesugi and Irvine, 1970) which are being used by Dr. James E. Hansen at the Goddard Institute for Space Studies, who is collaborating on this study.

Light undergoing multiple scattering by spherical particles becomes polarized in such a way that the polarization is a direct indication of the microstructure of the particles. Hence, if we want to determine the size distribution of the reflecting particles in a planetary atmosphere from the polarization characteristics of reflected sunlight, we can assume that the reflecting surface of the atmosphere under consideration is composed of spherical particles. It has been shown that the Venus clouds are composed of spherical particles (Hansen and Arking, 1971). This study can be applied most directly to Venus, where the cloud properties are still unresolved. Thus, by trying out several different simple models for types of scattering (e.g., Rayleigh, Mie, or some combination of the two for different optical depths) taking place in the Venusian clouds, and by comparing the resultant theoretical polarization with observations of polarization for Venus (Coffeen and Gehrels, 1969), some insight can be gained as to the physical nature of the Venusian clouds. Also, by studying the latitudinal-longitudinal variation of the polarization, a better picture of the horizontal inhomogenities of the Venus clouds may become available.

So far, intensity and polarization have been calculated for the cases of pure Rayleigh and pure Mie scattering. Currently, contour plots of these quantities are being constructed. The intensity values for Rayleigh scattering have been found to be in total agreement with an independent source (Sekera and Viezee, 1961).

A MICRODENSITOMETER ANALYSIS OF MARINER 6 AND 7 MULTICOLOR PHOTOMETRIC PHOTOGRAPHS OF MARS

by

Gregory L. Matloff

(Abstract of a paper submitted to Astronomical journal.)

A photometric analysis of Mariner 6 and 7 three-color (B, G, R) photographs of Meridiani Sinus, the South Polar region, and Hellas, is performed using a microdensitometer. Hellas is apparently more specular in nature than other Martian terrain features and the dark areas near the Martian South Polar cap appear much darker than dark regions near the equator. Although much of the difference is due to AGC effects, some of the difference may be due to the different natures of the two terrain types. Two hundred and thirty-three points

in Meridiani Sinus are mapped in at least one color and nine points are mapped in three colors. There is an apparent direct correlation between R/G reflectance ratio and height in the Meridiani Sinus region, based upon a comparison of R/G for four points in Meridiani Sinus and earth-based radar measurements of that region.

TECHNIQUE FOR PHOTOMETRIC DETECTION OF EXTRASOLAR PLANETS

by

Gregory L. Matloff and Alphonsus J. Fennelly*

(Abstract of a paper presented at a meeting of the American Optical Society in April 1972.)

O'Neill (1968) has discussed the possibility of building an interferometer array of mirrors in space having an optical resolution equivalent to that of a 5000 in. telescope. The applicability of such apparatus to detection and classification of extrasolar planets, using UBV photometry, has been discussed (Matloff, 1971). Utilizing Roman's (1959) estimate of the apparent magnitude of hypothetical planets circling Alpha-Centauri and O'Neill's discussion of the primary star's diffraction pattern, the S/N of the planet observed in the star's diffraction pattern and the photons received from the planet per unit time can be estimated. For an effective telescope diameter of 5000 in., S/N is about 0.1 for earthlike planets circling Alpha-Centauri and 0.01 for Tau-Ceti or Epsilon-Eridani. With an array of three widely separated 150 in. mirrors, about 100 photons sec^{-1} are received in the case of the planet circling Alpha-Centauri A in the V and B photometric channels and about 70 in the U. In the case of Tau-Ceti, or Epsilon-Eridani, the planet flux is about an order of magnitude lower, and 70 percent lower for Alpha-Centauri B. Although O'Neill's discussion was concerned with mirror arrays in space, it is possible to construct an earth-based optical interferometer in an arrangement similar to that used in radio astronomy (Swenson, 1969), using optical instead of electronic methods to correct for signal phase lag. If techniques of monitoring variations in the seeing can be developed, it may be possible to build an array of this type on a high terrestrial mountain instead of in space.

---

*American Elsevier Publishing Company, New York, New York.

ASYNCHRONOUS METEOROLOGICAL DATA INSERTION BY MEANS OF A COORDINATE TRANSFORMATION

by

Isidore M. Halberstam

Much progress was made during the past six months in testing the method of data initialization by using continuous asynchronous data only. To make this report comprehensible as an individual unit, a brief review of the problem and the proposed method of solution are necessary.

Introduction

In 1960, the Air Weather Service published a manual describing how weather analysts could best deal with reports submitted by air reconnaissance at times which were not simultaneous with standard synoptic reports. The advised procedure was to advect the data point, as well as possible, up to the time of synoptic reporting and to redraw the synoptic chart with the aid of the new data point. If a change in one of the readings (e.g., pressure) was indicated by changes in observed neighboring systems, the alteration was to be taken into account during advection. This procedure, as one could easily surmise, is highly subjective and is useful only if a small number of data points are available. But since large bodies of asynchronous data were not readily submitted at that time, these shortcomings were not considered crucial.

As the decade progressed, the problem of asynchronous data insertion took on a new meaning. With the advent of both satellite observations and numerical models of the atmosphere, the problem became one which involved large amounts of precious information which was needed as initial conditions for the numerical calculations. Satellites could cover areas which previously were devoid of observers such as the vast stretches of the South Pacific far from the shipping lanes. But they could not supply all their information at one time. Instead, they were able only to scan a comparatively small area at each point in their orbit. By the time they reached half-way around the earth, the data they had previously supplied was outdated and could not correctly be used in conjunction with later-supplied data. The numerical models, however, can only make use of data supplied for one particular time. It uses this information to produce a forecast. Any information supplied after the initial moment can no longer be used in the initial conditions, but will confront values produced by the model in its forecast. If the later information is similar to the forecast value, there is obviously no need for it, since the model apparently simulated nature well enough. If the observation is vastly different from the forecast, the model

has obviously done poorly, due perhaps to a poor knowledge of the initial field. One feels intuitively that the later-supplied information could help the model's forecast. Just how to make use of it most efficiently has produced recent research activity.

The most obvious procedure to handle asynchronous data is probably the simplest. It calls for simply inserting the data as it is received into its proper location. At each time-setp of the model, the satellite supplies data at a different grid point. If this data is forced into that grid point, the forecast will be altered. It was feared, however, that such a technique could not work if the neighboring grid points had forecast values which were different from the injected data. In that case, the detractors thought, an imbalance, or shock, would result and destroy the forecast. Jastrow and Halem (1970) attempted to demonstrate that such fears were unfounded. Their imaginative experiment showed that, to the contrary, inserted data would bring the computed values closer to the true solution and would cause no undue instabilities. Their experiment consisted of allowing the Mintz-Arakawa UCLA two-layer model to produce a forecast for a large number of days. The model was started again with the same conditions but after 119 days the forecast was interrupted and the entire field sprinkled with errors, both random and systematic. This caused the ensuing forecast to depart drastically from the original forecast. This departure was measured by the RMS error over the entire field of velocities. The model was allowed to run once more with the perturbations introduced at 119 days, but values from the original forecast were introduced at each time step at appropriate grid points. The RMS differences between the original and perturbed fields rapidly decreased to acceptable levels, even when the initial perturbation was extremely large. This would seem to indicate that raw satellite data could safely be inserted without too much difficulty into an ongoing numerical model and could substantially improve the forecast.

Morel, Lefevre, and Rabreau (1971), among others, found that Jastrow and Halem's results may not be universally applicable. They attributed the favorable results to the use of only one model in the experiment. The values used to simulate satellite data were values obtained from the same model during a previous run. Since the system was naturally attuned to these values, it could easily be guided back to producing values close to the original ones. If real data were to be inserted, or if a simpler model without too many degrees of freedom were employed, instabilities may very well occur. Besides, the adjustment period made short range forecasts turn out rather poorly, and a forecaster desiring a 12- or 24-hr forecast could not take advantage of the satellite data. To overcome these

disadvantages, Morel proposed an iterative scheme to perfect a 24- or 48-hr barotropic forecast. This involves inserting observed data at its appropriate time and space coordinates until the desired termination time is reached. At this point the program is reversed starting from the 24- or 48-hr forecast field and hindcasting to time 0 while again inserting the same data at its appropriate location. At time 0 the program is moved forward again, starting from the hindcast conditions, with data insertion taking place as before. The process should converge giving a desirable result after a few iterations. Despite its effectiveness, this method is severely limited from a practical standpoint. Aside from the philosophical problems involved in reversing supposedly irreversible physical processes, it is quite an expense to iterate a numerical model of some sophistication even for a short term forecast. Morel's test on a barotropic model is about as sophisticated as one can get without running up high expenses for computer time.

A series of other proposals for the assimilation of asynchronous data were presented at the Symposium on Four-dimensional Data Assimilation held at Princeton, N.J., in 1971. Some indicated that weighting factors could be used to ease the data into the model without creating unduly severe gradients or shock waves. Others contended that weighting the data does not reduce the RMS error to any substantial degree. A short survey of these presentations can be found in Kasahara (1972), and repetition here is unnecessary.

Coordinate transformation

All the above recommendations have one object in common. That is, they all suggest means to insert data into an already specified model. It is hoped that despite the poor initialization in the model a better forecast can be produced if accurate observations are fed consistently into the model. But this expectation may not be borne out in a large number of cases. When simpler models are used, the introduction of new data may create the feared shock waves by constructing sharp gradients in the vicinity of the insertion. In sophisticated models, smoothing mechanisms or pseudo-viscosity terms can help keep the unstable modes in check while allowing the influence of the inserted data to spread. The ability to cope with the instabilities becomes, then, highly dependent on the type of numerical method employed.

Current research seems to be moving away from smoothing and pseudo-viscosity toward implicit methods of solution. What effect insertion may have on these schemes is unknown, and no general conclusions can be drawn no matter how many schemes are tested. The reason for this lies in the mathematics of insertion. From the point of view of mathematics, once sufficient initial and boundary conditions are specified, the solutions to the differential equations of the model are

determined. Any "new" information is extraneous and can only be accepted if that information is compatible with the determined solution. If the information is not commensurate with the solution, the field is over-specified and either some of the specifications must be rejected or the solution will not exist. The same holds true when inserting data into a numerical model. Since initial conditions are given, later insertion can only be considered overspecification. The only reason investigators have found success in data insertion experiments is that they are working with numerical analogs rather than analytical equations. These allow the inserted data to usurp the role of the initial conditions and slowly replace the solution based on the original conditions with the solution derived from the inserted data. Thus, it is hoped that the model will reject the first specification and keep the specification due to the inserted data. Analytically, however, this is still over-specification and can lead to destruction of the solution. It is like trying to solve six equations for five unknowns. If no two equations are linearly dependent, no solution can exist. The only way to insure a solution is to remove one of the specifications.

To overcome the problem of "overspecification", it may be worthwhile to initialize the field in a manner different from traditional methods. All investigators admit that the initial field based on poor observations ought to be modified by later observations based on satellite measurements. But calculations cannot begin unless there is some initial field. So, although sparse data is available over large portions of the globe for any given time, interpolations and extrapolations are performed based on data in neighboring areas. The later, more reliable data must then overcome the initial poor specification before the forecast can be made more reliable. If, however, the initial data could be ignored, and the later data, asynchronous though it may be, serve as the new "initial" field, the forecast may then be more reliable to begin with. This may be accomplished by means of a coordinate transformation in time. The satellite data is asynchronous, i.e., it is a function of space and time. It can be made synchronous if the time coordinate, t, is exchanged for a new coordinate, τ, which is also dependent on space and time. It is constructed to coincide with the satellite path, so that all the data is furnished at the line $\tau = 0$ and is hence "initial". This coordinate is completely analogous to the σ-coordinate invented by atmospheric model builders to compensate for topographic features which could affect the traditional vertical coordinates z and p. The τ-coordinate should accomplish the same task by smoothing out the "bumps" in the initial data curve. Thus, if data is given along a curve $G(t,x,y) = 0$, or, alternatively $t = T(x,y)$, we may devise a time coordinate $\tau = t - T(x,y)$ (or $t/T(x,y)$ so that $\tau = 0$ (or 1) along the data curve, and the curve can indeed serve as initial data in the new coordinate system.

The coordinate transformation will, of course, alter the equations. If numerical means of solution are employed, it may be necessary to alter the scheme to fit the new terms. Truncation errors may increase if additional derivatives are necessary. On the other hand, stability requirements may be relaxed if coefficients appear that can have the effect of shortening the time step.

As an example, consider the equation:

$$\frac{\partial P}{\partial x} = \frac{\partial P}{\partial t} + P$$

in dimensionless variables, with initial condition $P(x,0) = 4x\,[\exp(.5x)]$. The solution here is $P(x,t) = 4(x + t)\exp[.5(x - t)]$. If information were not available at $P(x,0)$ but along some curve $P(x,t(x))$, where $t(x) = 2\sqrt{x}$, say, we could still determine a solution to the equation. If we transform coordinates, such that (x,t) is replaced by (ξ,τ), where $\xi = x$ and $\tau = t - 2\sqrt{x}$, we get a new equation in terms of ξ and τ:

$$\frac{\partial P}{\partial \xi} = \frac{\partial P}{\partial \tau}\left(\frac{1 + \sqrt{\xi}}{\sqrt{\xi}}\right) + P .$$

Now, however, the condition that was specified along $P(x,t(x))$ is a condition at $P(\xi,0)$ which appears as an ordinary initial condition in (ξ,τ) coordinates. The solution obtained should still be the same but will be in terms of (ξ,τ) instead of (x,t). Of course, the transformation can be used to express the solution in terms of (x,t) if necessary.

An experiment was performed using the numerical analog of this equation. Results of the experiment were described in the previous report submitted in December 1971.

The wave equation

A similar experiment was conducted with the wave equation and with a one-dimensional gravity wave equation. The wave equation was first used in its one-dimensional form and then as a two-dimensional equation. The results proved similar in both cases, so only the two-dimensional equation will be discussed here. The wave equation is in the well-known form

$$c^2\frac{\partial^2\phi}{\partial x^2} + c^2\frac{\partial^2\phi}{\partial y^2} = \frac{\partial^2\phi}{\partial t^2}\,, \qquad \text{(1a)}$$

where c represents the phase speed of the wave. Its form is well-known, and the scheme is conditionally stable. If i refers to the time index, J, the x-index, and ℓ, the y-index, the numerical equation is:

$$c^2 \frac{\phi^i_{j+1,\ell} - 2\phi^i_{j,\ell} + \phi^i_{j-1,\ell}}{(\Delta x)^2} + \frac{c^2}{(\Delta y)^2}(\phi^i_{j,\ell+1} - 2\phi^i_{j,\ell} + \phi^i_{j,\ell-1})$$

$$= \frac{\phi^{i+1}_{j,\ell} - 2\phi^i_{j,\ell} + \phi^{i-1}_{j,\ell}}{(\Delta t)^2} \tag{1b}$$

The exact solution to the equation depends on the initial and/or boundary conditions. In this experiment, the boundary and initial conditions were chosen to coincide with a solution equal to

$$\phi(x,y,t) = 3 \sin .01(x - ct) + 3 \sin .01(y - ct) \tag{2}$$

The transformed equation looks rather complicated because of the second order derivatives. The transformation was given as $\xi = x$, $\eta = y$, and $\tau = t - 2\sqrt{x + y + 15}$. In the (ξ, η, τ) coordinate system the equation becomes:

$$c^2 \left\{ \frac{\partial^2 \phi}{\partial \xi^2} + \frac{\partial^2 \phi}{\partial \eta^2} + 2 \frac{\partial^2 \phi}{\partial \tau \partial \xi} \frac{\partial \tau}{\partial x} + 2 \frac{\partial^2 \phi}{\partial \tau \partial \eta} \frac{\partial \tau}{\partial y} + \frac{\partial \phi}{\partial \tau} \left(\frac{\partial^2 \tau}{\partial x^2} + \frac{\partial^2 \tau}{\partial y^2} \right) \right\}$$

$$= \frac{\partial^2 \phi}{\partial \tau^2} \left\{ c^2 \left[\left(\frac{\partial \tau}{\partial x} \right)^2 + \left(\frac{\partial \tau}{\partial y} \right)^2 \right] + 1 \right\} \tag{3a}$$

Some difficulty was encountered trying to find the numerical analog to this equation. Unlike the first-order equation, this equation has cross derivatives between time and space. To use purely centered differences would somehow involve using an implicit scheme since there would be more than one variable at the i + 1 time step. This is technically feasible but the increased computation time and the difficulty of the programming would make the original equation much more appealing than the transformation. To avoid this, a backward difference was used on the cross-terms so that there was only one variable to be solved at i + 1. But this also increased the truncation error considerably. However, when a second iteration was performed using the values generated by the backward differencing and employing a strictly centered differencing, the truncation error was reduced considerably. The numerical equation for the first iteration was then:

$$c^2\Bigg\{\frac{\phi^{i}_{j+1,\ell} - 2\phi^{i}_{j,\ell} + \phi^{i}_{j+1,\ell}}{(\Delta\xi)^2} + \frac{\phi^{i}_{j,\ell+1} - 2\phi^{i}_{j,\ell} + \phi^{i}_{j,\ell-1}}{(\Delta\eta)^2}$$

$$+ 2\frac{\phi^{i+1}_{j,\ell} - \phi^{i+1}_{j-1,\ell} - \phi^{i-1}_{j,\ell} + \phi^{i-1}_{j-1,\ell}}{4\,\Delta\tau\,\Delta\xi}\frac{\partial\tau}{\partial x}$$

$$+ \frac{2}{4\Delta\tau\,\Delta\eta}\left(\phi^{i+1}_{j,\ell} - \phi^{i+1}_{j,\ell-1} - \phi^{i-1}_{j,\ell} + \phi^{i-1}_{j,\ell-1}\right)\frac{\partial\tau}{\partial y} + \frac{\phi^{i+1}_{j,\ell} - \phi^{i-1}_{1,\ell}}{2\,\Delta\tau}\left(\frac{\partial^2\tau}{\partial x^2} + \frac{\partial^2\tau}{\partial y^2}\right)\Bigg\}$$

$$= \frac{\phi^{i+1}_{j,\ell} - 2\phi^{i}_{i,\ell} + \phi^{i-1}_{i,\ell}}{(\Delta\tau)^2}\left(1 - c^2(\tau_x^2 + \tau_y^2)\right) \qquad (3b)$$

The only unknown quantity here is $\phi^{i+1}_{j,\ell}$. All others, including $\phi^{i+1}_{j-1,\ell}$ and $\phi^{i+1}_{j,\ell-1}$, are known from previous time steps. The second iteration affects only the third and fourth terms on the left hand side where $\phi^{i+1}_{j,\ell}$ and $\phi^{i-1}_{j,\ell}$ receive the indeces j+1 and ℓ+1.

To compare results, the transformation was used to transform values from different τ-times to t-times. Since values were available only at finite steps in τ most values obtained were only close to, but not exactly equal to, the real time t. However, since the time step used was rather small, this should not be noted as a significant cause for departure. Parameters used in the calculation were $c = .8$, $\Delta t = .9$, $\Delta x = \Delta y = 2.1$. The third part of the experiment involved data insertion after perturbing the initial field with random errors equal to $\pm$ 1/8 the values of the initial field. The insertion was done similarly to the manner discussed in the previous report. The results in terms of average absolute truncation errors for a few time steps are shown in Table I. (Truncation error here is simply the difference between the exact solution and the numerical solution).

As can be seen, the centered difference method using exact initial conditions allows for the lowest truncation errors with a very slow growth rate of these errors. The results using equation (3b) gives truncation errors two orders of magnitude larger than the results using equation (1b). This is due to three factors: First, as mentioned before, the backward differencing causes an increase in truncation error; second, there are more terms with derivatives adding to the total; third, the coefficient of the time derivative on the right-hand side of (3b) magnifies the time step $\Delta\tau$. This term is less than one, which is the same as multiplying $\Delta\tau$ by a number more than one, which will increase the truncation

Table I. Average Absolute Errors for ϕ

Time	Centered differencing (1b) x 10^{-6}	Asynchronous, no iteration (3b) x 10^{-4}	Asynchronous, one iteration x 10^{-6}	Data insertion
49.50	3.0363	3.6101	5.8603	20.207
50.40	3.0820	3.6966	6.0537	20.635
51.30	3.1255	3.7824	6.2489	21.041
52.20	3.1668	3.8673	6.4454	21.422
53.10	3.2057	3.9513	6.6435	21.780
54.00	3.2423	4.0344	6.8426	22.117
54.90	3.2764	5.1164	7.0425	22.432
55.80	3.3080	4.1974	7.2432	22.724
56.70	3.3371	4.2773	7.4444	22.986
57.60	3.3636	4.3559	7.6461	23.222
58.50	3.3874	4.4333	7.8481	23.439
59.40	3.4085	4.5094	8.0502	23.633
60.30	3.4269	4.5841	8.2524	23.794
61.20	3.4425	4.6574	8.4544	23.934
62.10	3.4553	4.7292	8.6561	24.056
63.00	3.4652	4.7995	8.8573	24.159
63.90	3.4722	4.8682	9.0578	24.226
64.80	3.4763	4.9352	9.2575	24.274
65.70	3.4774	5.0006	9.4564	24.317
66.60	3.4756	5.0642	9.6543	24.335

error while requiring stricter linear instability criteria. The iteration procedure reduces the errors to the same order of magnitude as equation (1b), but the rate of error growth is still larger. For the data insertion method, the shock effect is quite evident since the errors are from three to four times the size of the variable. The solutions obtained without inserting data, in fact, were better behaved and their departure was not as great. This seems to indicate that at least in simple models, without any sophisticated damping devices, the threat of shock waves being created is quite real when raw data is inserted. Using the transformed coordinates, however, circumvents this problem.

One-dimensional free surface gravity waves

A test experiment was performed on primitive barotropic equations whose variables depended only on x. The linear counterpart of this model is discussed by Kurihara (1965). The equations used here are:

$$\frac{\partial u}{\partial t} + mu\frac{\partial u}{\partial x} = fv - \frac{\partial \phi}{\partial x} \tag{4a}$$

$$\frac{\partial v}{\partial t} + mu\frac{\partial v}{\partial x} = - fu \tag{4b}$$

$$\frac{\partial \phi}{\partial t} + mu\frac{\partial \phi}{\partial x} = vfU - m(gH + \phi)\frac{\partial u}{\partial x} \tag{4c}$$

where u is the westerly component of velocity, v is the southerly component, f is the Coriolis parameter, U is the average westerly component (16 m sec^{-1}), $H(y)$ is the mean height of the free surface ($5800 - \frac{fU}{g}y$), m is the map factor, and ϕ is the deviation of geopotential from the mean. m and f depended only on the y-direction while u, ϕ and v only varied in the x-direction. The numerical scheme employed was the same employed by Shuman (see Haltiner, 1971, p. 227) with simplifications made for the one-dimensional case. We shall use Shuman's notation which, briefly summarized, gives:

$$\bar{A}^{x} \equiv \tfrac{1}{2}(A_{j+\frac{1}{2}} + A_{j-\frac{1}{2}}),\quad A_x \equiv \frac{1}{\Delta x}(A_{j+\frac{1}{2}} - A_{j-\frac{1}{2}})$$

and so

$$\bar{A}^{xx} = \tfrac{1}{4}(A_{j+1} + 2A_j + A_{j-1}),\quad \bar{A}^{x}_{x} = \frac{1}{2\Delta x}(A_{j+1} - A_{j-1})$$

The numerical analog of (4) is given by

$$u_t^{-t} = -\overline{\bar{m}^{x-x}\bar{u}^{x-x}u_x + \bar{f}^{x-x}\bar{v}^{x-x} - \phi_x}^{\,x} \tag{5a}$$

$$v_t^{-t} = -\overline{\bar{m}^{x-x}\bar{u}^{x-x}v_x - \bar{f}^{x-x}u}^{\,x} \tag{5b}$$

$$\phi_t^{-t} = -\overline{\bar{m}^{x-x}\bar{u}^{x-x}\phi_x + \bar{v}^{x-x}\bar{f}^{x-x}U - \bar{m}^{x}(gH + \bar{\phi}^{x})u_x}^{\,x} \tag{5c}$$

The second term on the right of (5c) is equivalent to the first term on the right in (4c) and is derived from the equality $vg\frac{\partial H}{\partial y} = - fvU$ which defines the dependency of H on y. The averaging symbol over m and f is academic in this model, since they do not vary in the x-direction. Using a time step of five minutes and $\Delta x = \Delta y = 200$ km, forecasts were made for 12, 24, 36, and 48 hr, and the heights $H + \frac{\phi}{g}$ were plotted by the S-D 4060 plotter at the Goddard

Institute for Space Studies (GISS) in New York City. Extra smoothing was inserted every 50 time steps to keep the curves smooth and to avoid any instabilities that might arise. The initial conditions were simple sinusoidal waves for all three variables with their respective ranges as $12 \leq u \leq 20$, $-\frac{2\pi}{9} \times 9.8 \leq v \leq \frac{2\pi}{9} \times 9.8$, $-980.0 \leq \phi \leq 980.0$. The boundaries in the x-direction were cyclic so that the last grid points always coincided with the first.

The experiment was conducted in the same manner as the previous ones, but since no exact solution was available here, the results of equation (5) were used as the true solution and as data for the initialization of the asynchronous equations and for insertion during the third part of the experiment.

For the asynchronous experiment, the transformation was given in analytical terms. The transformation was

$$\tau = t + 1 - 10^{-3}(x + y)$$

This coincides with a satellite speed of approximately 1 km sec^{-1}. The transformed equations were then:

$$\frac{\partial u}{\partial \tau} = [\dot{\tau}(-mu \frac{\partial u}{\partial \xi} + fv - \frac{\partial \phi}{\partial \xi}) - \tau_x(fUv - mu \frac{\partial \phi}{\partial \xi} - m(gH + \phi) \frac{\partial u}{\partial \xi})]/D \qquad (7a)$$

$$\frac{\partial \phi}{\partial \tau} = [-mu \frac{\partial v}{\partial \xi} - fu]/\dot{\tau} \qquad (7b)$$

$$\frac{\partial \phi}{\partial \tau} = [\dot{\tau}(-mu \frac{\partial \phi}{\partial \xi} + fUv - m(gH + \phi) \frac{\partial u}{\partial \xi}) - \tau_x(f(gH + \phi)\, mv - m^2 u(gH + \phi) \frac{\partial u}{\partial \xi} - m(gH + \phi) \frac{\partial \phi}{\partial \xi}]/D \qquad (7c)$$

where $D \equiv \dot{\tau}^2 - m\tau_x^2(gH + \phi)$, $\dot{\tau} \equiv 1 + mu \frac{\partial \tau}{\partial x}$, $\tau_x \equiv \frac{\partial \tau}{\partial x}$

The numerical counterpart of (7) is exactly similar to (5), since τ and D were calculated separately and are not involved in the smoothing of the products. Computation was carried out until all grid points had been calculated up to 48 hr of real time. An interpolation was used to recover the fields of u, v, and ϕ at 12, 24, 36, and 48 hr of real time. The interpolation consists of using equation (6) to test at each τ-step if the value of τ coincided with $t = 12$ hr, say. When that value of t was located between two values of τ, a linear interpolation was carried out which estimated the asynchronous value of the variable for the required time. If larger time steps are used, or if the fields undergo quick change, better methods of interpolation may be necessary. The same method was

employed (in reverse) to derive the field at $\tau = 0$, when the field at all t was known.

The boundaries in the asynchronous case gave another sort of problem. Since the boundaries were assumed cyclic for the synchronous case, it was desired to keep them cyclic in the asynchronous case. However, for any given τ-step it was no longer true that the last grid points have the same value as the first ones, since, by equation (6) they were not at the same real time. It was easy enough to define the "later" boundaries from earlier ones, but the reverse was virtually impossible unless some sort of implicit scheme or iterative method was performed. In practice, the boundaries were determined by interpolating from the synchronous results at each time step. This did not upset the solution too badly, nor did it nudge the results closer to the true ones to any degree.

The third part of the experiment involved perturbing the initial field by random errors which, in magnitude, were 25 percent of the velocities and $\pm$ 100 m for the height field. Data was inserted at each time step according to equation (6) by setting $\tau = 0$. The set of grid points at each time step that coincided with the x and y values derived were fed interpolated data. This meant that at each time step, a diagonal swath of grid points received information until the entire field was covered in about 2.5 hr. The results of the experiment are shown in Figures 1-13. The choppiness in the asynchronous graphs is due mainly to the interpolation. Otherwise, the angles and troughs are accurately depicted at all times. The data insertion, as expected, does poorly in the early forecasts but improves toward the end of the period, although no new data is inserted after the initial 2.5 hr. This is due in part to the smoothing which serves the dual purpose of cancelling out the random errors and spreading the influence of the inserted data. It is also due to the nature of the fixed slope in the y-direction which tends to act as a forcing function in equation (4c) so that by 48 hours the data insertion method gives nearly the same results as the error-free model.

For a numerical comparison, values for u are given in Table II at grid points $\ell = 7$, $j = 19$-21, for times 0, 12, and 36 hr. Notice how once again the insertion method does better for the long-range forecast than for short-range. The effect of smoothing in cancelling the random errors can be seen by the improvement of the results where there was no insertion whatsoever.

Note on smoothing

Special mention must be made regarding the effect of smoothing on the different techniques. By smoothing properly, it is hoped, the high frequency computational modes can be damped while the important long-wave physical mode is allowed to survive. Here, the same smoothing algorithm was used for both the synchronous

Table II. Values of u(m sec^{-1}) for different times at L = 7, 19 ≤ J ≤ 21

Time (hr)		0	12	36
	j = 19	12.763	9.320	-10.442
Synchronous	20	13.323	9.320	-10.442
(no error)	21	14.000	9.491	-11.096
	19	- - -	9.191	-10.295
Asynchronous	20	- - -	9.181	-10.733
	21	- - -	9.895	-11.023
Initial	19	13.777	7.585	-10.056
Random error	20	13.254	7.534	- 9.653
(no insertion)	21	11.943	8.396	-10.080
	19	13.777	7.622	-10.451
Data insertion	20	13.254	8.470	-10.508
	21	11.943	9.312	-11.111

and asynchronous case. It was originally feared that such a procedure would create serious deviations because different data would be incorporated in each case. In the synchronous case, smoothing balances the value at a grid point with the values found in neighboring points at a given time. In the asynchronous case, the values in neighboring grid points are not values given at the same real time. Therefore, smoothing in the asynchronous case means smoothing in time as well as space. When excess smoothing was induced, the values began to diverge, in fact. The contours appeared flattened after 12 hr in both cases, but the values of the contours were significantly different. With the reduction of extra smoothing to only once every 50 time steps, the correlation improved drastically as can be seen from the plots. In the case of the insertion method on the other hand, increased smoothing brought the results in line much more quickly, for the reasons previously mentioned. Thus smoothing seems to be a damping technique which is beneficial to the insertion of data technique but detrimental to the coordinate transformation method.

Conclusions and proposals

The results so far in this investigation have seemed very promising and call for future research. The work on the first order equation and the wave equation prove that shock waves are a threat in data insertion. The free surface equations show that data insertion is not useful for short-range forecasts, while the transformation procedure shows definite promise of being able to handle prediction from the time the entire field is covered.

The next step in this research will be to undertake, as much as possible, a simulated procedural run using the asynchronous transformation. The two-dimensional barotropic equations will be used for a small region on the Shuman grid. Initial conditions, boundary conditions, and satellite data will be gleaned from the six-layer model of Shuman. The results will be analyzed both from a comparison of 500-mb plots and from a comparison of error indicators such as the RMS error.

Acknowledgment

Much appreciation is given to Mr. R. Karn of the Goddard Institute for Space Studies for his valuable assistance in arranging and managing a rather complicated program.

Fig. 1. PHI(X,Y) BY SYNCHRONOUS METHOD WITHOUT RANDOM ERRORS

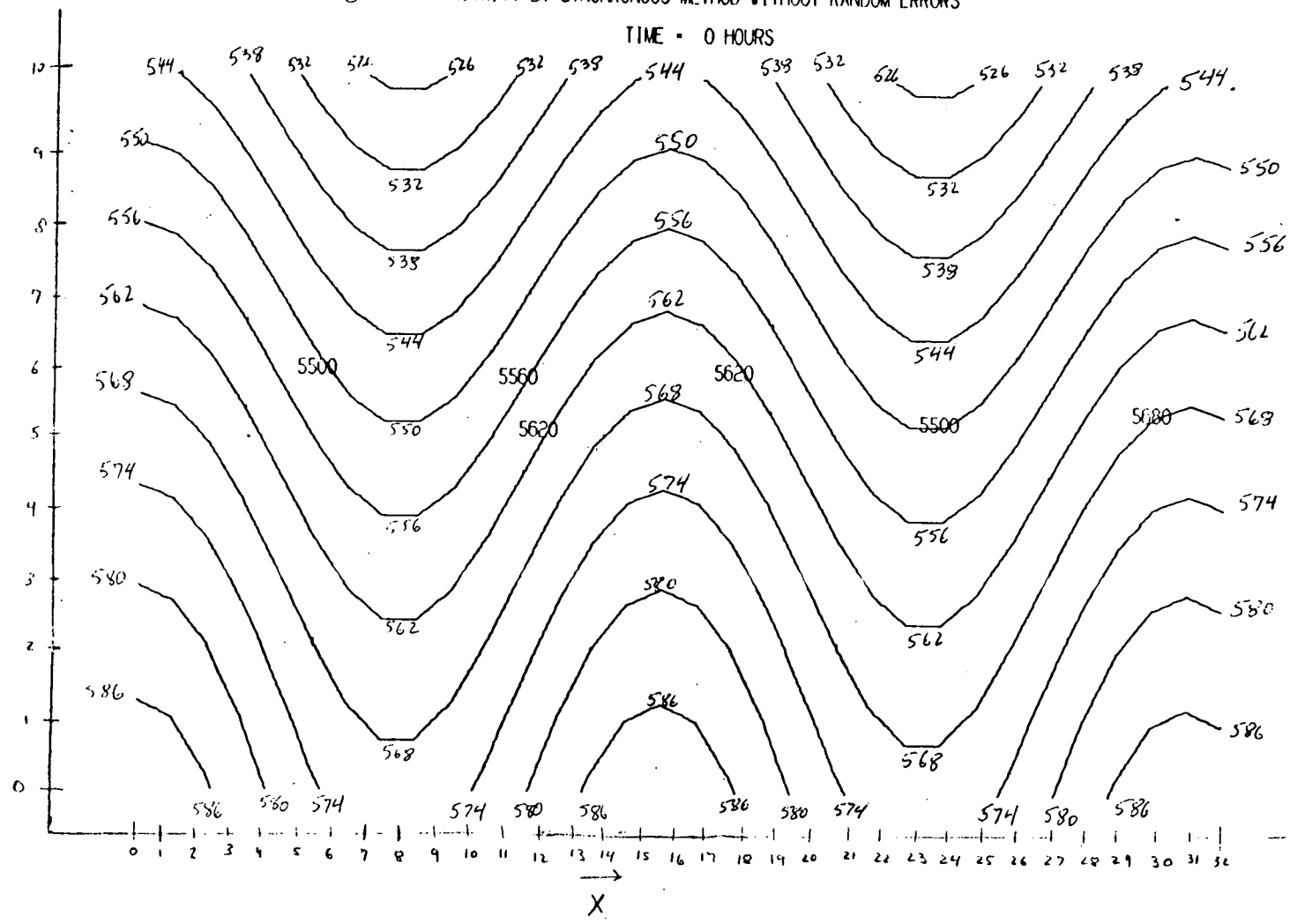

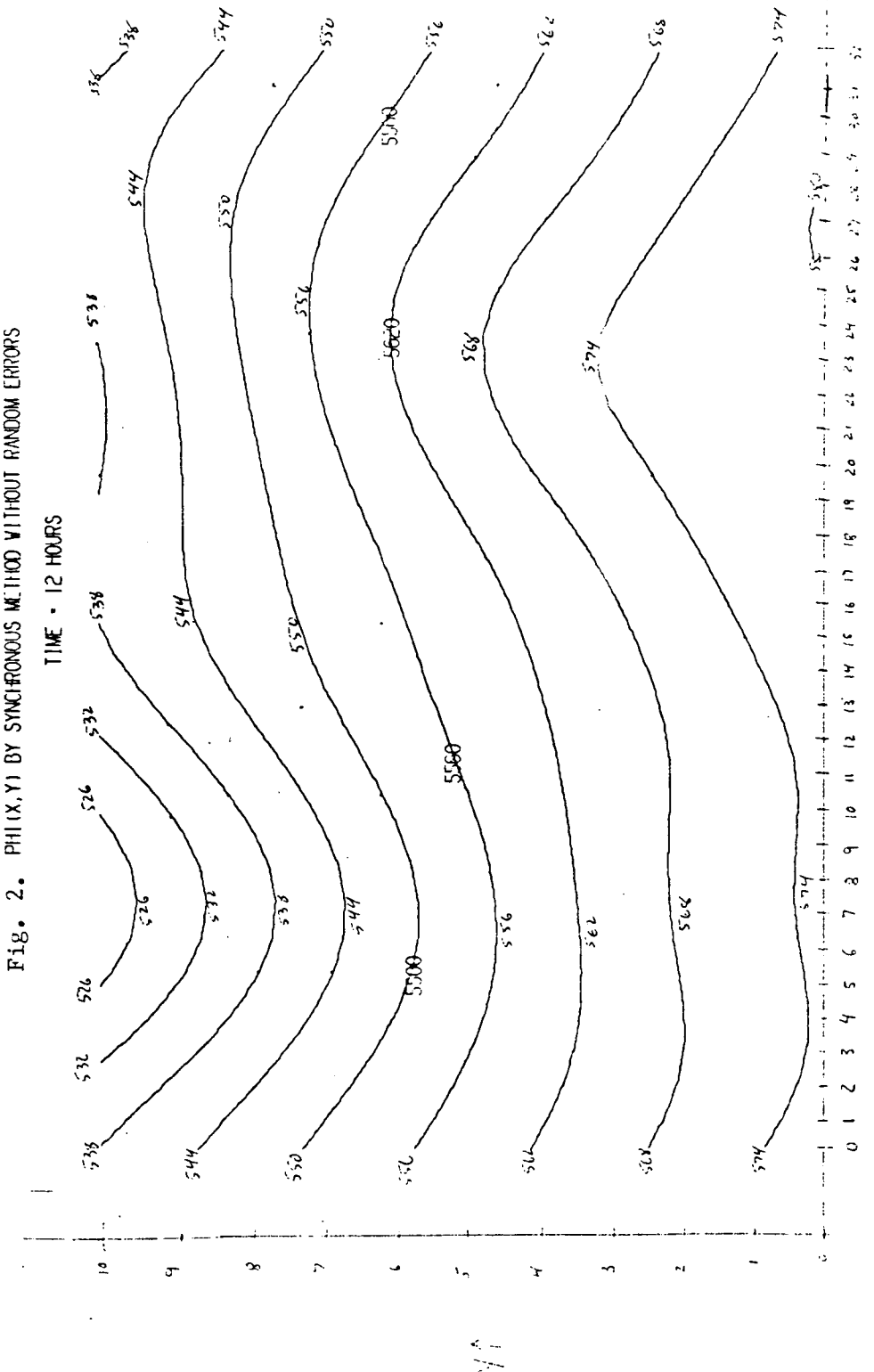

Fig. 2. PHI(X,Y) BY SYNCHRONOUS METHOD WITHOUT RANDOM ERRORS

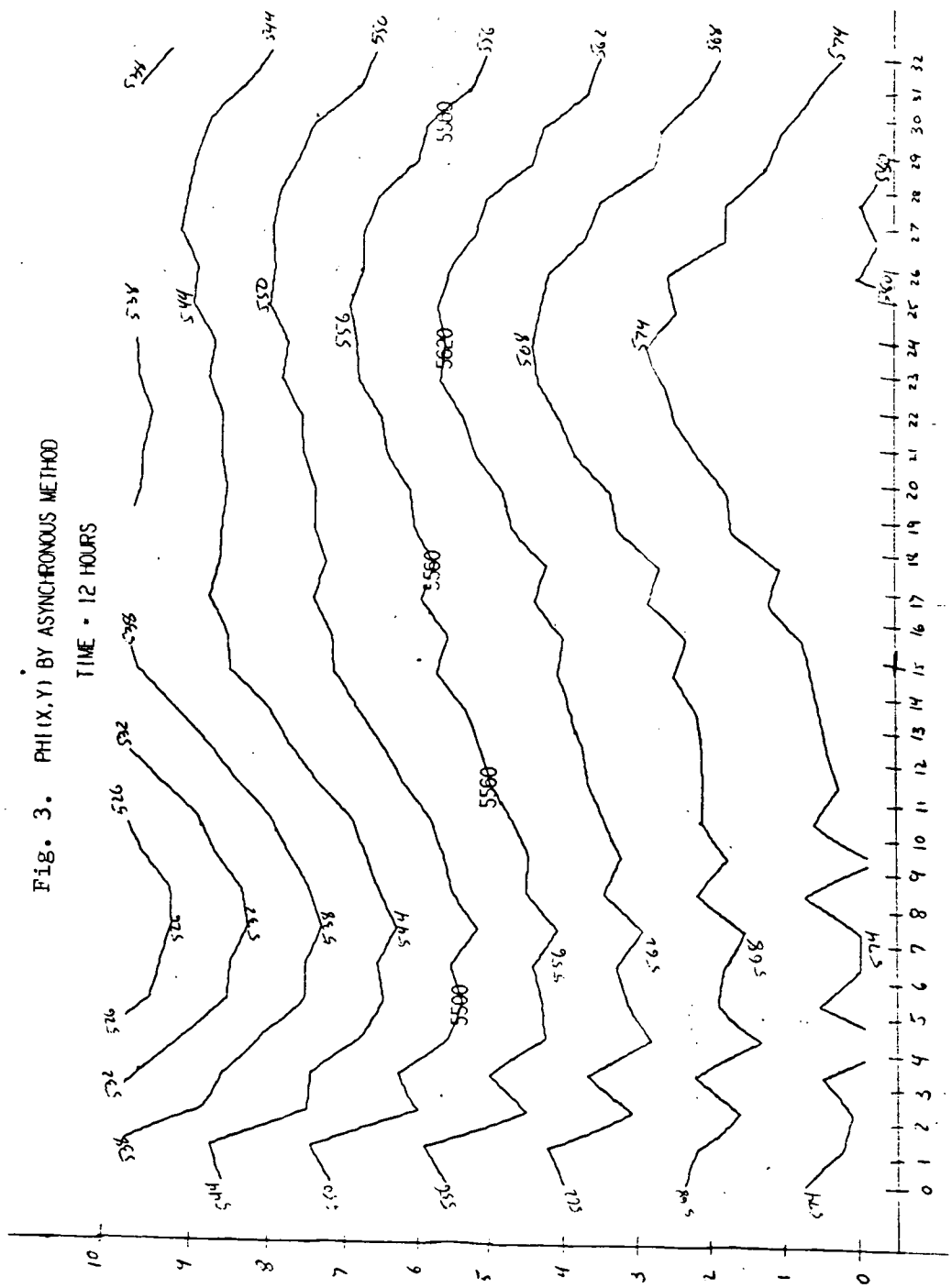

Fig. 3. PHI(X,Y) BY ASYNCHRONOUS METHOD

TIME = 12 HOURS

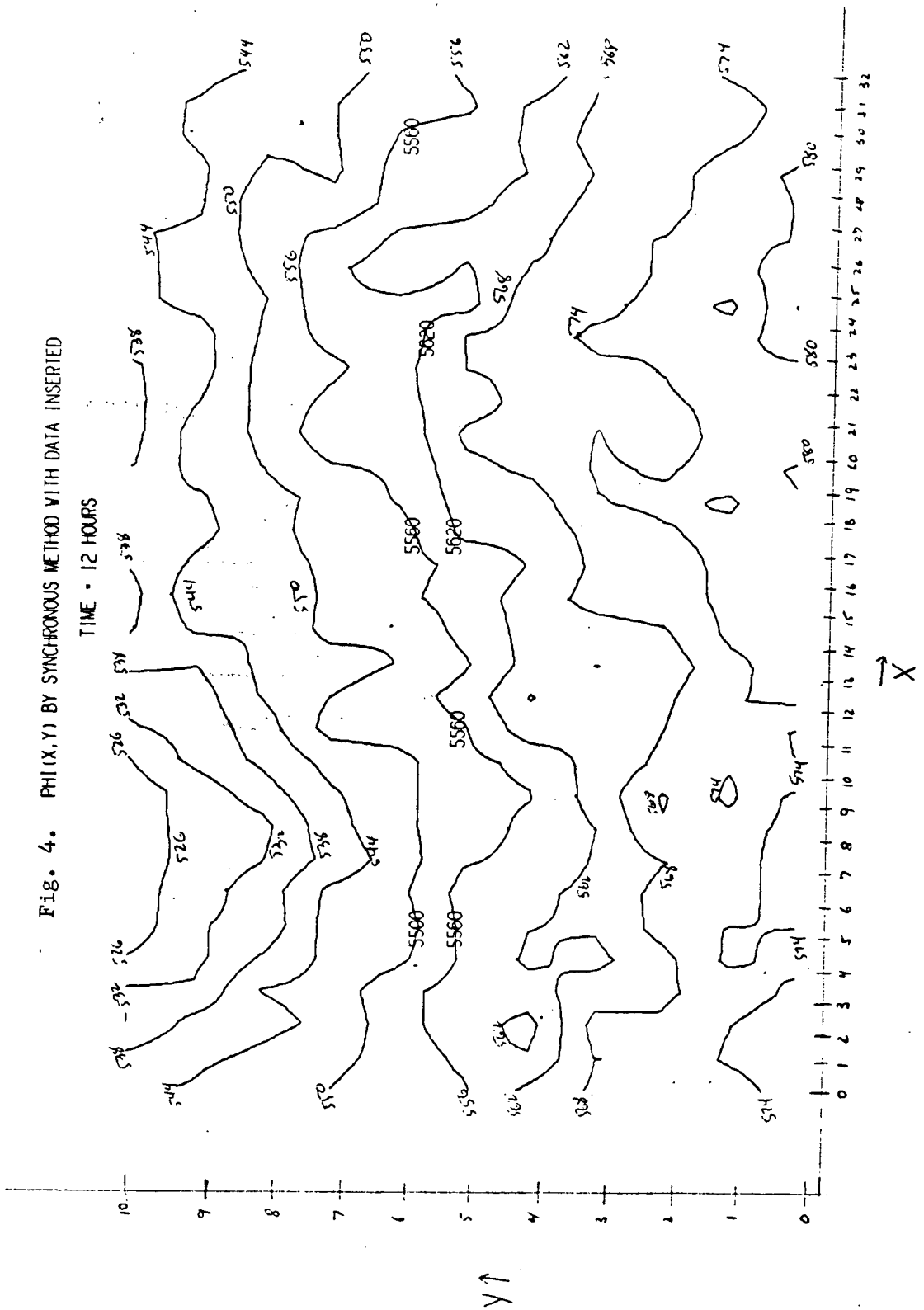

Fig. 4. PHI(X,Y) BY SYNCHRONOUS METHOD WITH DATA INSERTED
TIME = 12 HOURS

Fig. 5. PHI(X,Y) BY SYNCHRONOUS METHOD WITHOUT RANDOM ERRORS

TIME = 24 HOURS

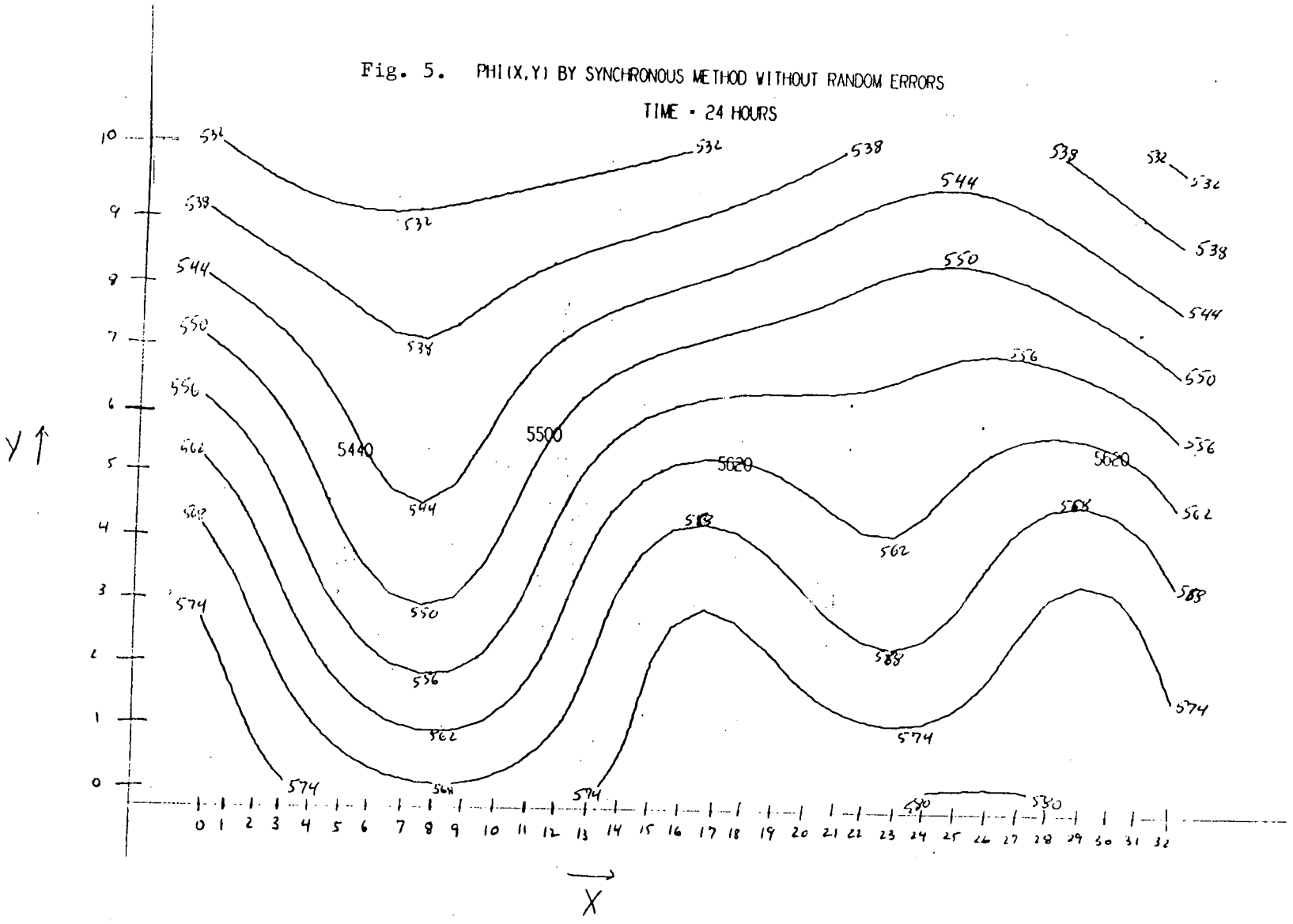

Fig. 6. PHI(X,Y) BY ASYNCHRONOUS METHOD

TIME = 24 HOURS

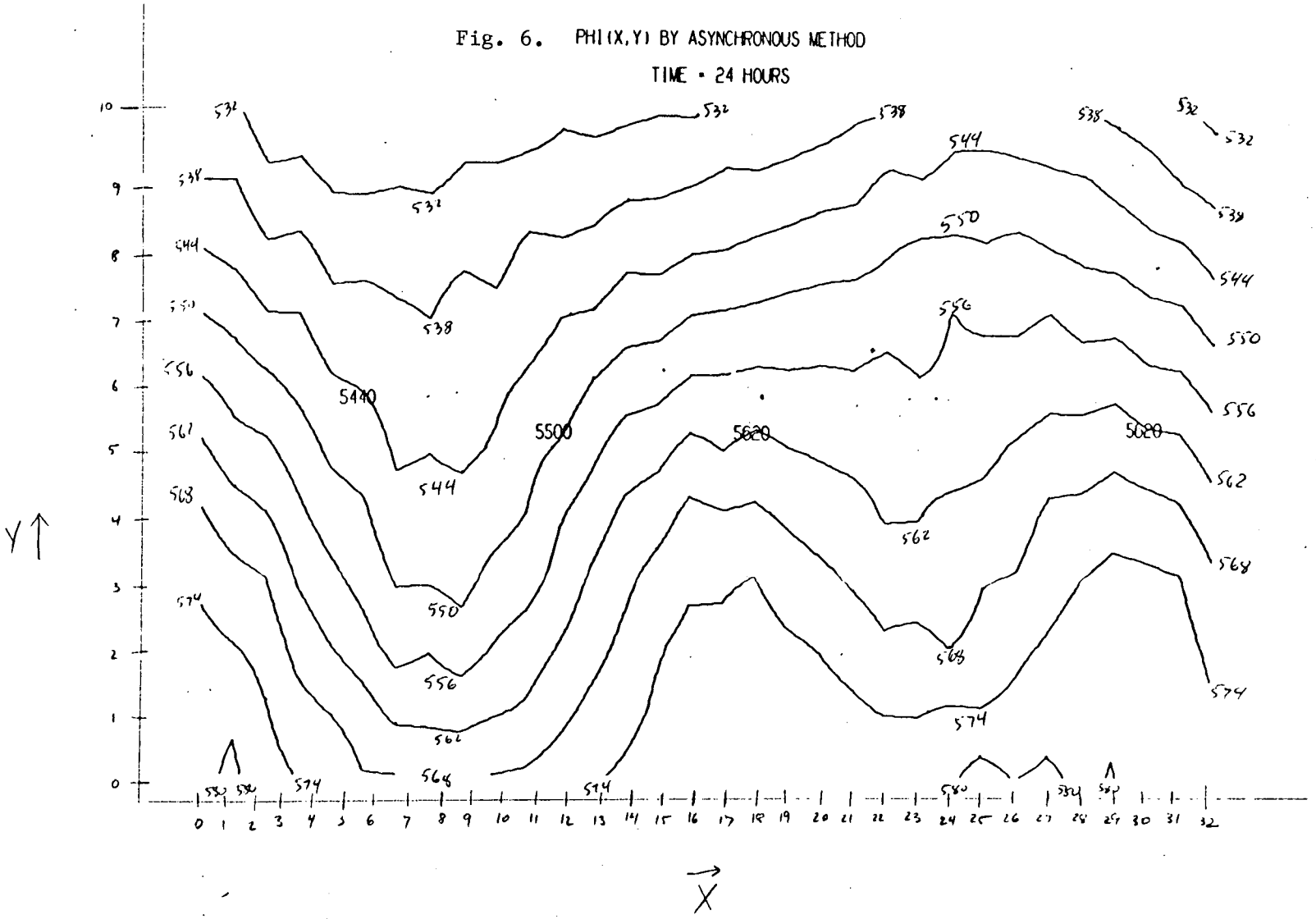

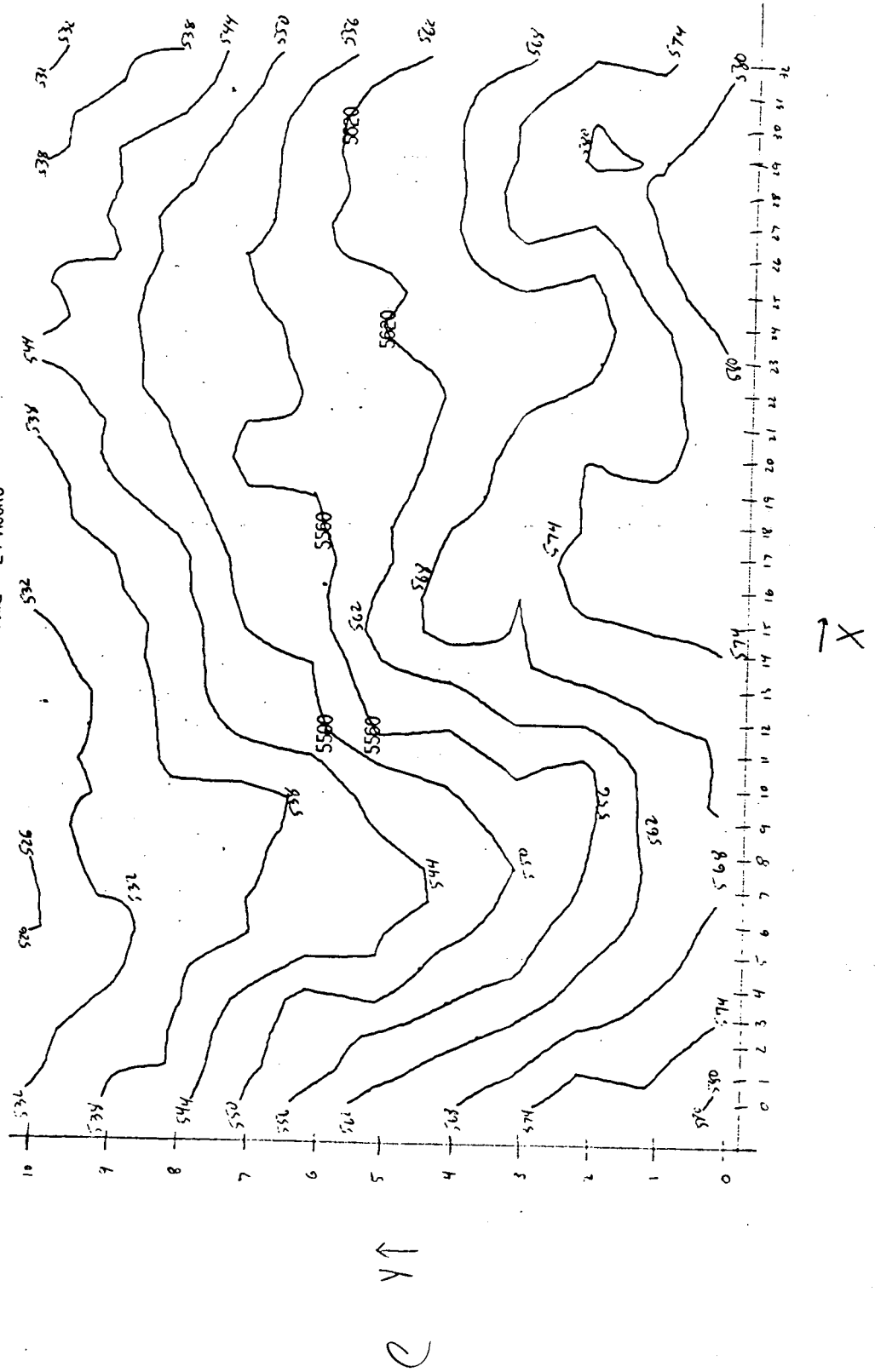
PHI(X,Y) BY SYNCHRONOUS METHOD WITH DATA INSERTED
TIME = 24 HOURS
5500
5560
5620
5680
Y
X

Fig. 7.

Fig. 8. PHI(X,Y) BY SYNCHRONOUS METHOD WITHOUT RANDOM ERRORS

TIME = 36 HOURS

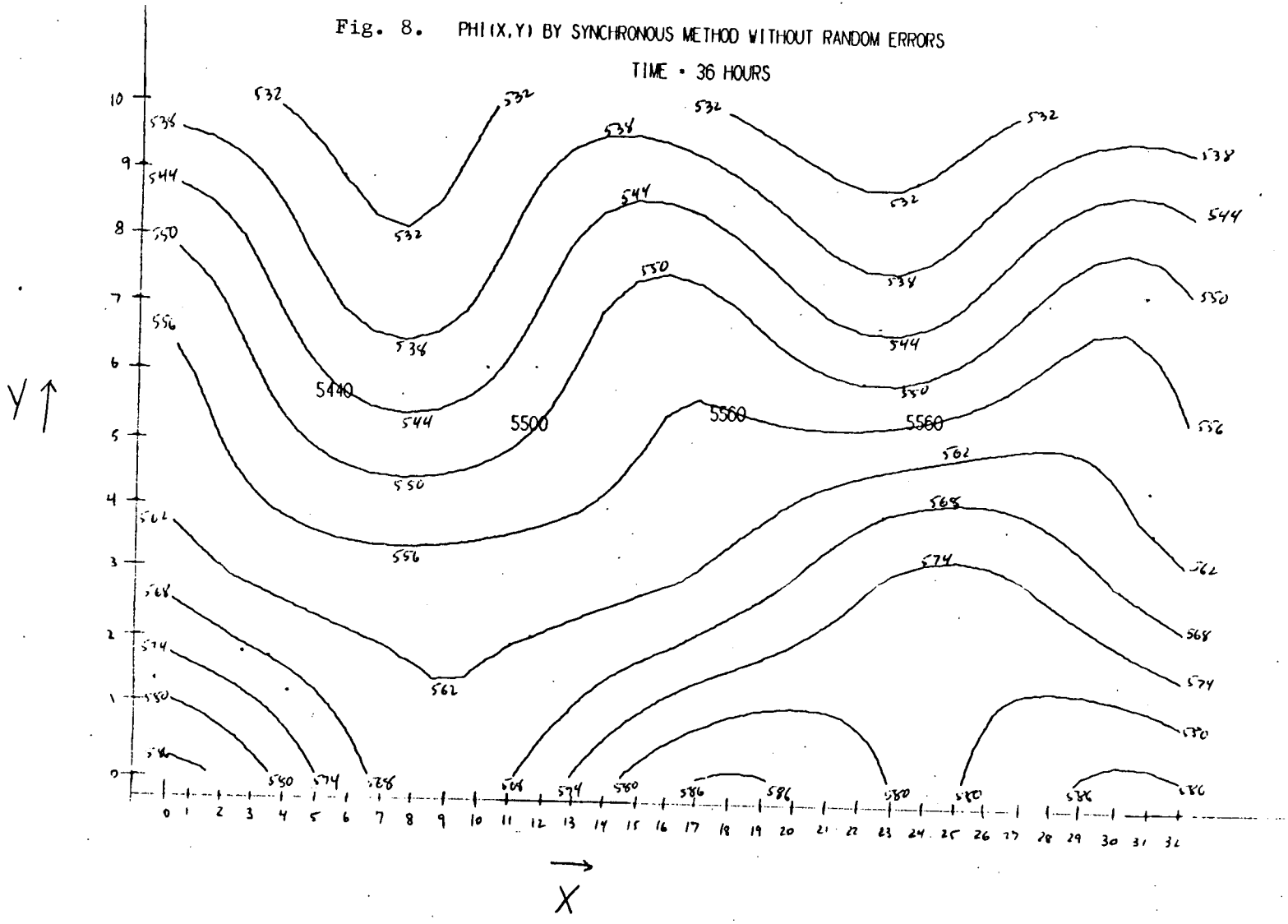

Fig. 9. PHI(X,Y) BY ASYNCHRONOUS METHOD

TIME = 36 HOURS

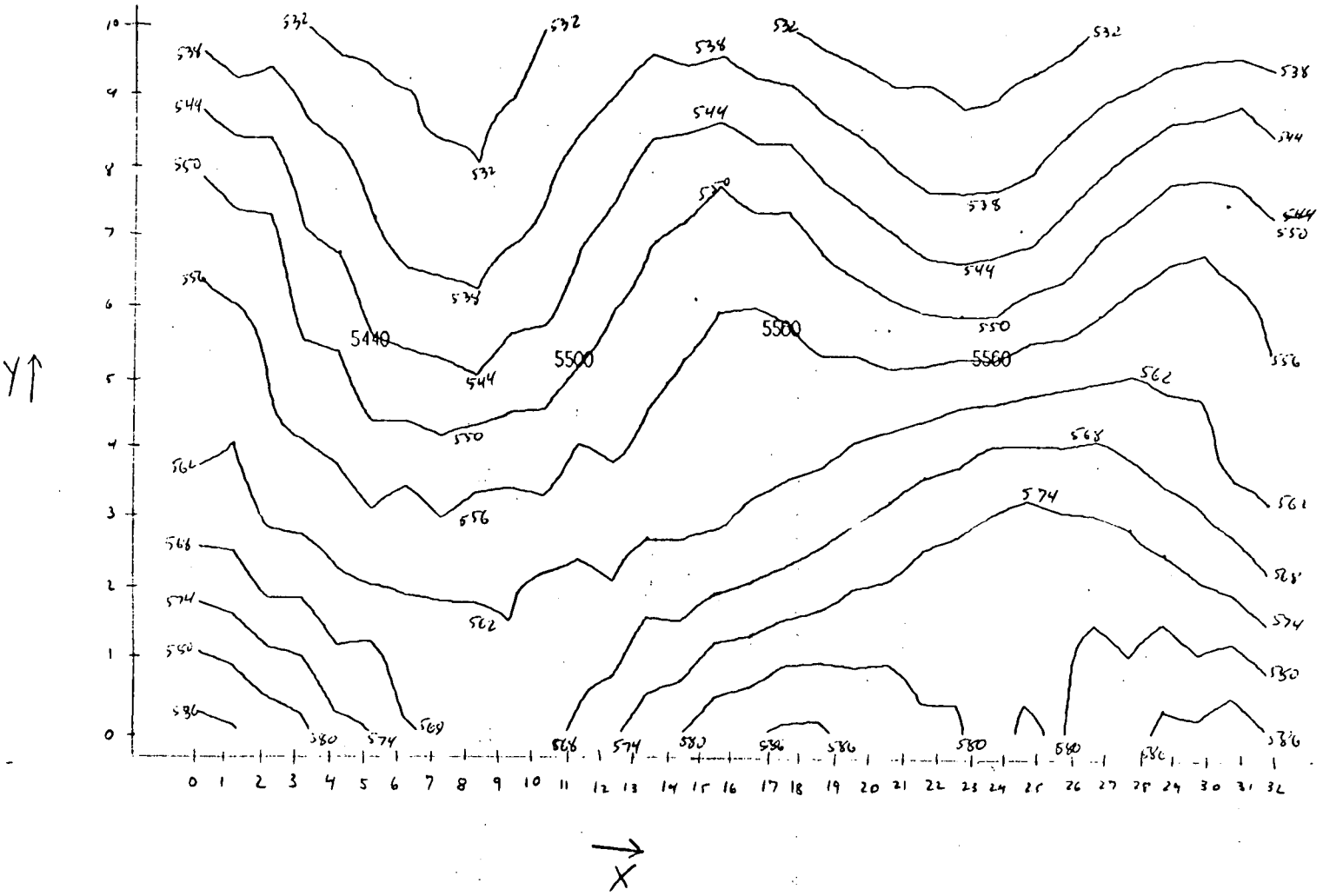

Fig. 10. PHI(X,Y) BY SYNCHRONOUS METHOD WITH DATA INSERTED

TIME = 36 HOURS

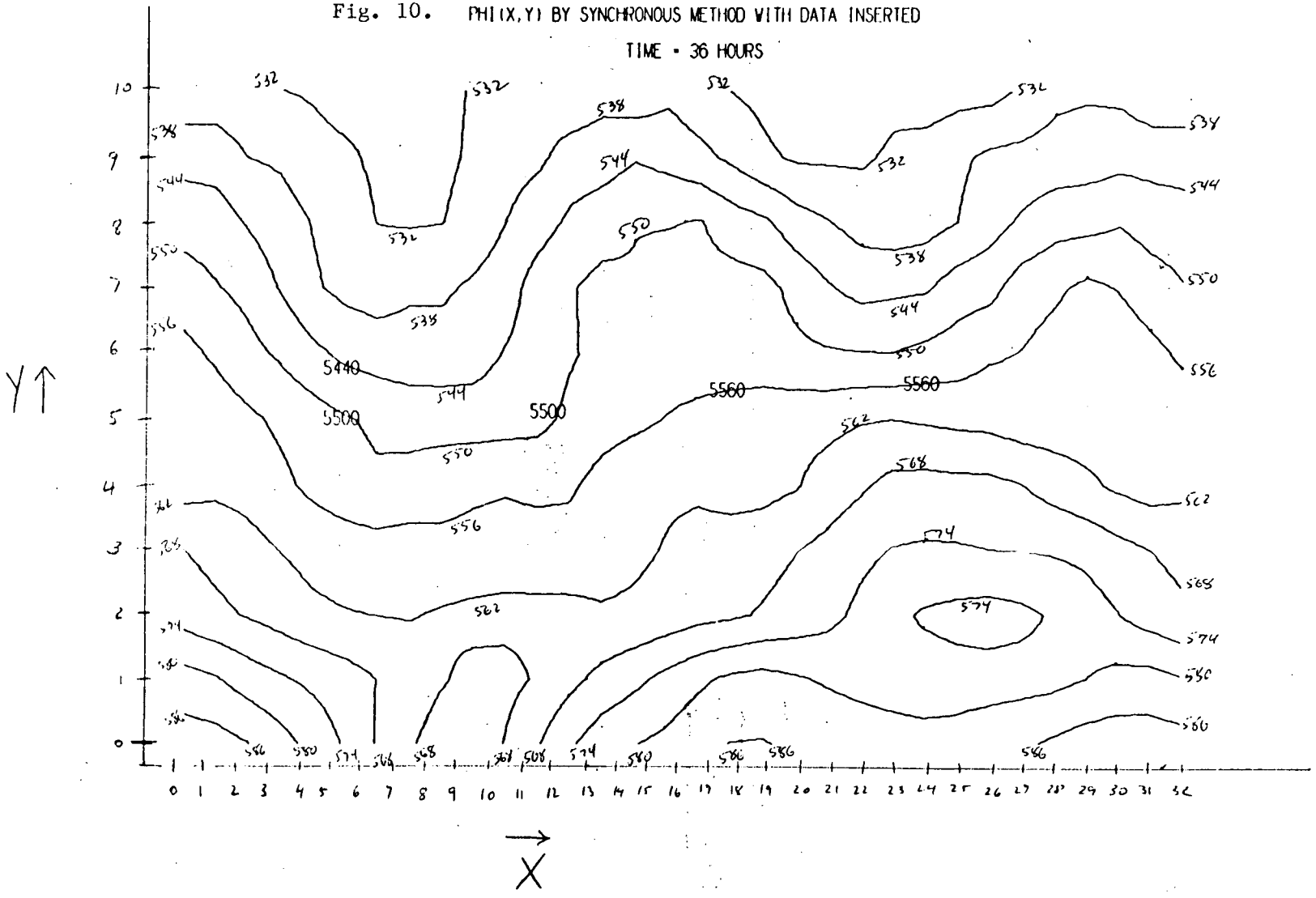

Fig. 11. PHI(X,Y) BY SYNCHRONOUS METHOD WITHOUT RANDOM ERRORS

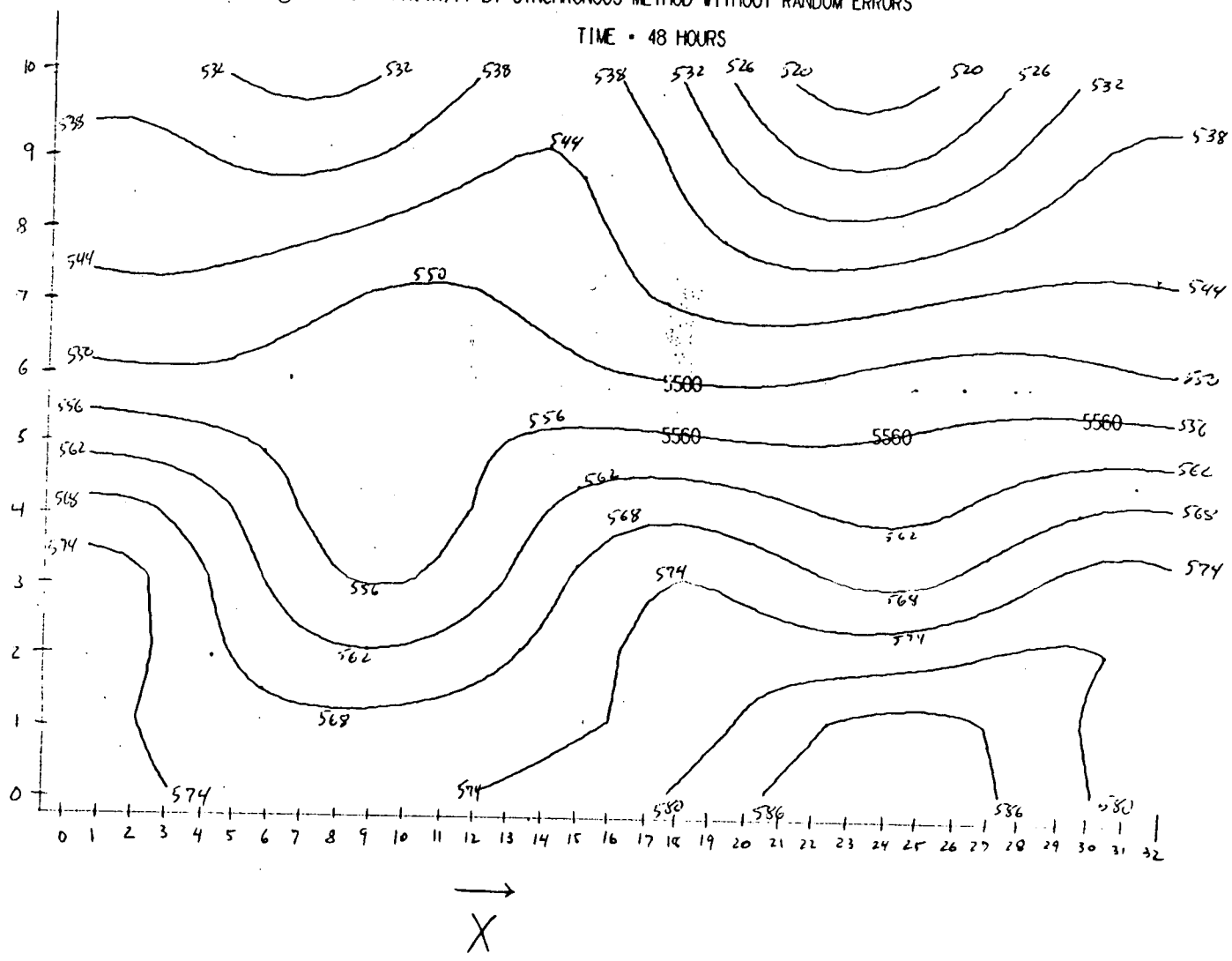

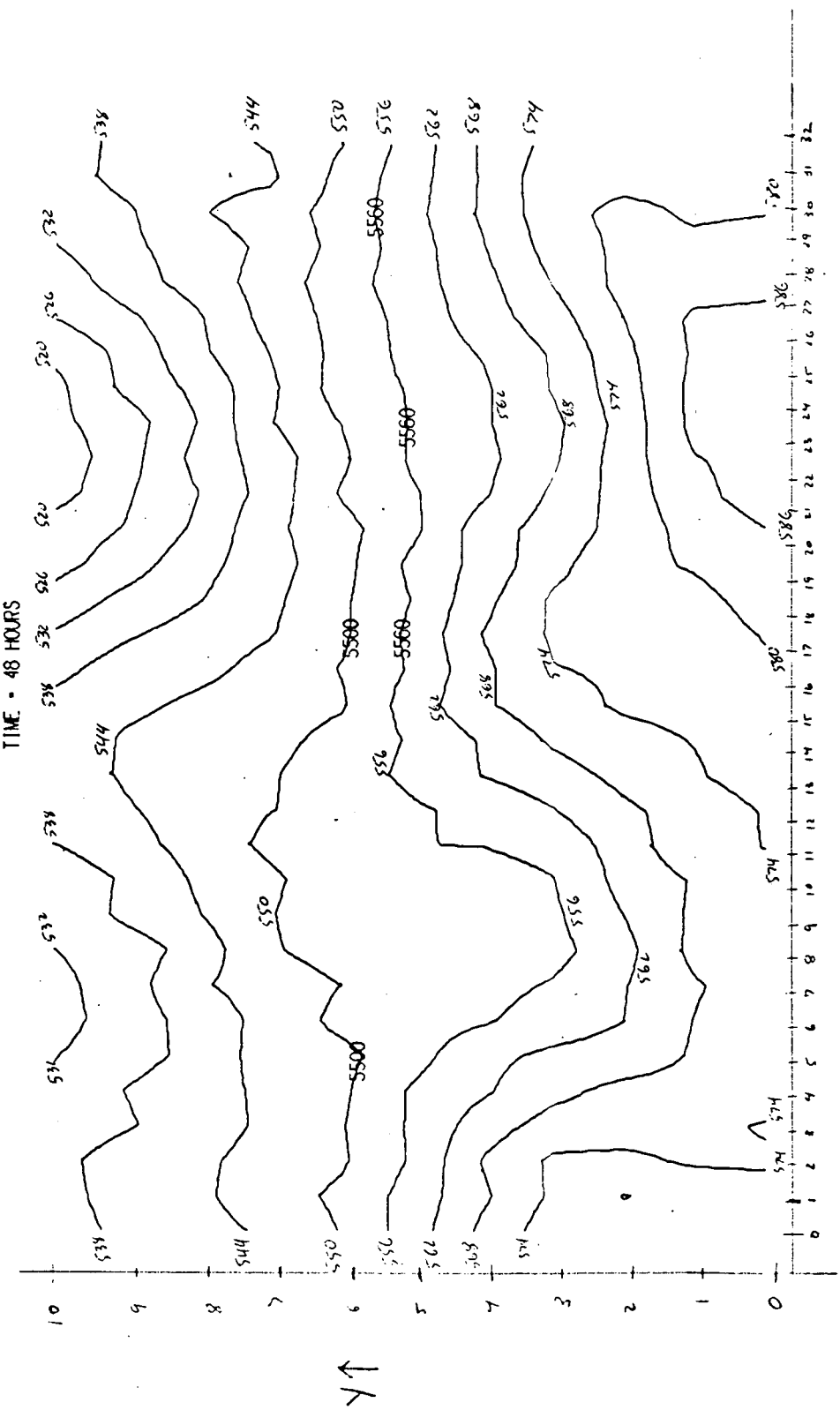

Fig. 12. PHI(X,Y) BY ASYNCHRONOUS METHOD
TIME = 48 HOURS

Fig. 13. PHI(X,Y) BY SYNCHRONOUS METHOD WITH DATA INSERTED

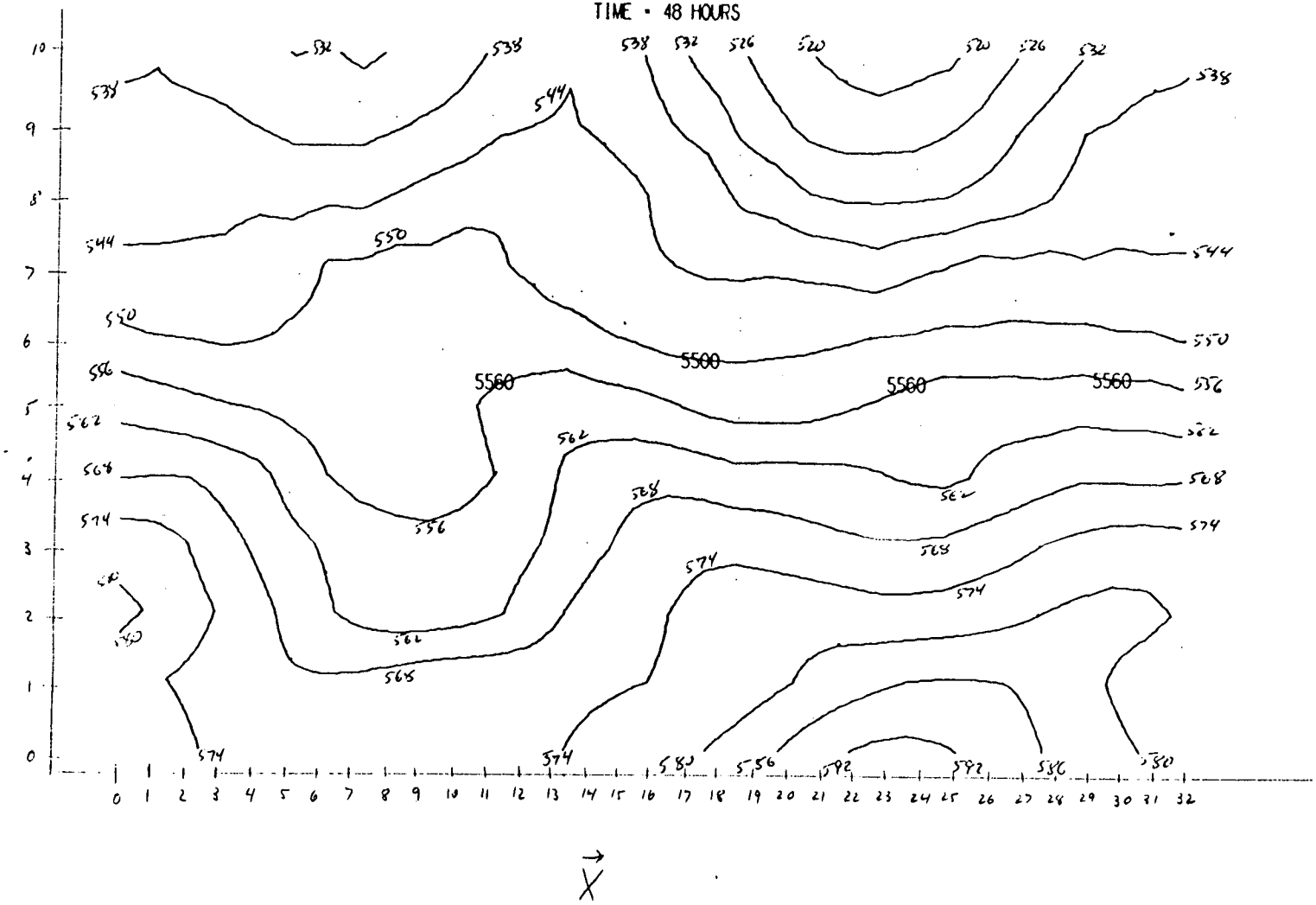

REFERENCES

Air Weather Service, 1960: Use of asymptotic data in analysis and forecasting. AWSM 105-10, U. S. Air Force.

Arakawa, H., 1969: World survey of climatology, v. 8: Climates of Northern and Eastern Asia. Elsevier Publishing Co., Amsterdam, 248 pp.

Chahine, Moustafa T., 1968: Determination of the temperature profile in an atmosphere from its outgoing radiance. J. Opt. Soc. Amer., v. 58, pp. 1634-1637.

Coffeen, D. L., and T. Gehrels, 1969: Wavelength dependence of polarization XV: Observations of Venus. Astron. Journ., v. 74, pp. 433-445.

Critchfield, Howard, 1966: General climatology. Prentice Hall, pp. 394-401.

Haltiner, George J., 1971: Numerical weather prediction. John Wiley and Sons, New York.

Hansen, James E., 1971: Multiple scattering of polarized light in planetary atmospheres. Part I. The Doubling method. J. Atm. Sci., v. 28, pp.120-125.

Hansen, James E. and Albert Arking, 1971: Clouds of Venus: Evidence for their nature. Science, v. 171, pp. 669-672.

Hogan, Joseph S., 1972: Personal communication.

House, Frederick B., 1968: Clouds and the inversion problem. J. Quant. Spectros. and Rad. Trans., v. 8, pp. 69-83.

Jastrow, R. and M. Halem, 1970: Simulation studies related to GARP. Bull. Amer. Meteor. Soc., v. 51, pp. 490-513.

Kasahara, Akira, 1972: Simulation experiments for meteorological observing systems for GARP. Bull. Amer. Meteor. Soc., v. 53, pp. 252-264.

King, Jean I. F., 1964: Inversion of slabs by varying thicknesses. J. Atm. Sci., v. 21, pp. 324-326.

Kunihara, Y., 1965: On the use of implicit and iterative methods for the time integration of the wave equation. Mon. Wea. Rev., v. 93, pp. 33-46.

Matloff, Gregory L., 1971: Icarus, v. 15, p. 341.

Miller, Albert, and Jack C. Thompson, 1970: Elements of meteorology. Charles E. Merrill Publishing Co., Columbus, Ohio, pp. 374-381.

Meeks, M. L., and A. E. Lilley, 1963: The microwave spectrum of oxygen in the earth's atmosphere. J. of Geophys. Res., v. 68, pp. 1683-1703.

Morel, P., G. Lefevre, and G. Rubreau, 1971: On initialization and non-synoptic data assimilation. Tellus, v. 23, pp. 197-206.

O'Neill, Gerard K., 1968: A high-resolution orbiting telescope. Science, v. 160, pp. 843-7.

Roman, N. G., 1959: Astronomical Journal, v. 64.

Sekera, Zdenek and William Viezee, 1961: Distribution of the intensity and polarization of diffusely reflected light over a planetary disk. Report prepared for U. S. Air Force Project Rand, R-389-PR, 45 pp.

Staelin, David H., 1969: Passive remote sensing at microwave wavelengths. Proc. IEEEE, v. 57, pp. 427-439.

Smith, W. L., P. K. Rao, R. Koffler, and W. R. Curtis, 1970: The determination of sea surface temperature from satellite high resolution infrared window radiation measurements. Mon. Wea. Rev., v. 98, pp. 604-611.

Swenson, C. W., Jr., 1969: Annual review of astronomy and astrophysics, v. 2, pp. 353-373.

Uesugi, A., and W. M. Irvine, 1970: Multiple scattering in a plane-parallel atmosphere. I. Successive scattering in a semi-infinite medium. Astrophys. Journ., v. 159, pp. 127-135.

U. S. Department of Commerce, 1969a: Monthly Climatic Data for the World., v. 22.

U. S. Department of Commerce, 1969b: Climates of the World, 28 pp.

van de Hulst, H. C., 1963: A new look at multiple scattering. Unpublished, pp. 59-70.

Wallen, C., 1970: World survey of climatology, v. 5: Climates of northern and western Europe. Elsevier Publishing Co., Amsterdam, 252 pp.

Wark, D. Q., and H. E. Fleming, 1966: Indirect measurements of atmospheric temperature profiles from satellites: 1. Introduction. Mon. Wea. Rev., v. 94, pp. 351-362.

FINANCIAL STATEMENT

(Including University Contribution)

Balance on hand, 30 November 1971	$16,594
Additional funds received 1972	70,000
Total	$86,594

Expended

December 1971	$ 1321.
January 1972	1953.
February 1972	3555.
March 1972	3008.
April 1972	3528.
May 1972	3608.
Total	$16,973

Balance on hand, 31 May 1972.	$69,621

James E. Miller
Principal Investigator